tert-Butyl as a Functional Group: Non-Directed Catalytic Hydroxylation of Sterically Congested Primary C−H Bonds

Siu-Chung Chan,[1] Andrea Palone,[1] Massimo Bietti[2]* and Miquel Costas[1]*

[1]Institut de Química Computacional i Catàlisi (IQCC) and Departament de Química, Universitat de Girona; Campus Montilivi, Girona E-17071, Catalonia, Spain.

[2]Dipartimento di Scienze e Tecnologie Chimiche, Università "Tor Vergata"; Via della Ricerca Scientifica, 1 I-00133 Rome, Italy.

*Corresponding authors Email: bietti@uniroma2.it, miquel.costas@udg.edu

Abstract: The *tert*-butyl group is a common aliphatic motif extensively employed to implement steric congestion and conformational rigidity in organic and organometallic molecules. Because of the combination of a high bond dissociation energy (~ 100 kcal mol^{-1}) and limited accessibility, in the absence of directing groups, neither radical nor organometallic approaches are effective for the chemical modification of *tert*-butyl C–H bonds. Herein we overcome these limits by employing an electron-poor manganese catalyst, [Mn(^{CF3}bpeb)(OTf)$_2$], that operates in the strong hydrogen bond donor solvent nonafluoro-*tert*-butyl alcohol (NFTBA) and catalytically activates hydrogen peroxide to generate a powerful manganese-oxo species that effectively oxidizes *tert*-butyl C−H bonds. Leveraging on the interplay of steric, electronic, medium and torsional effects, site-selective and product chemoselective hydroxylation of the *tert*-butyl group is accomplished with broad reaction scope, delivering primary alcohols as largely dominant products in preparative yields. Late-stage hydroxylation at *tert*-butyl sites is demonstrated on 6 densely functionalized molecules of pharmaceutical interest. This work uncovers a novel disconnection approach, harnessing *tert*-butyl as a potential functional group in strategic synthetic planning for complex molecular architectures.

Introduction

Because of the biological and pharmaceutical significance of oxygenated hydrocarbon frames and of the opportunities offered by C(sp^3)−O bonds for follow-up chemical elaboration, C(sp^3)−H bond oxygenation is an extensively investigated transformation[1-6]. Selecting among multiple non-equivalent C−H bonds in organic molecules, and in particular targeting stronger bonds over weaker and intrinsically more activated ones, stand as some of the main challenges associated to the development of C−H functionalization methods[7-13]. Such transformations would make accessible so far unconsidered paths allowing the streamlined synthetic elaboration of organic molecules.

From a thermodynamic perspective, the reactivity trend operating in hydrogen atom transfer (HAT) reactions mediated by radical and radical-like reagents such as metal-oxo species is greatly influenced by the C−H bond dissociation energies (BDEs) that typically follow the order: tertiary > secondary >> primary (**Scheme 1A**)[14]. In contrast, in precious metals mediated C(sp^3)−H bond functionalization proceeding through the formation of an organometallic intermediate, an opposite reactivity trend is observed, dictated by the strength of the resultant M−C bond (**Scheme 1B**)[15-18].

The *tert*-butyl group is a common molecular motif used to implement steric hindrance and structural rigidity in organic and organometallic molecules[19]. However, in terms of reactivity, the *tert*-butyl C−H bonds represent a special case. The singular combination of high BDE and steric encumbrance make *tert*-butyl C−H bonds generally unreactive against both HAT and organometallic operating reagents[13,20,21]. In addition, in the presence of these structural units, 'chain walking' reactions cannot be employed due to the impossibility of M−H migration through the *tert*-butyl quaternary carbon[22-24]. As a result, there is a lack of synthetic methodology for the non-directed selective functionalization of *tert*-butyl C−H bonds, and the synthetic potential of this transformation has been so far overlooked.

Interestingly, the oxidation of *tert*-butyl C−H bonds of bioactive molecules has been reported in enzymatic reactions involving iron oxygenases that operate via hypervalent iron-oxo species[25,26], suggesting that these species may be suitable oxidants to address this challenging problem. Manganese complexes bearing aminopyridine ligands are powerful catalysts that, in the presence of hydrogen peroxide, oxidize C(sp^3)−H bonds via reaction mechanisms that resemble oxygenases and entail HAT executed by hypervalent manganese-oxo species[27-30]. Structural and electronic tuning of these catalysts, combined with medium effects[31-34] can be employed to manipulate the chemoselectivity of the reaction, offering a powerful tool for selective functionalization. We have recently described that these complexes effectively catalyze the intramolecular γ-lactonization of primary C−H bonds in carboxylic acid substrates (**Scheme 1C**)[35,36]. On the other hand, the intermolecular oxidation of a substrate such as 2,2,3,3-tetramethylbutane was only accomplished in very low yield (<2%), in line with state-of-the-art oxidations with bioinspired catalysts[37-39].

We envisioned that the electrophilicity of the oxidizing manganese-oxo species could be enhanced by catalyst design and medium effects exerted by the solvent[40,41]. Building on these ideas, herein we disclose site-selective and product chemoselective hydroxylation of *tert*-butyl C−H bonds using a bioinspired manganese catalyst and aqueous hydrogen peroxide as the oxidant in the strong hydrogen bond donor (HBD) solvent nonafluoro-*tert*-butyl alcohol (NFTBA) (**Scheme 1E**). We show that the synergistic cooperation of different factors operating in the HAT step may be used to achieve high levels of selectivity in the hydroxylation of *tert*-butyl C−H bonds in substrates containing multiple functionalities. Understanding of these factors and their rational application provides valuable guidelines for expanding the scope of non-directed C(sp^3)−H oxidation reactions. The reaction installs a primary alcohol adjacent to a *gem*-dimethyl motif and serves as an orthogonal approach for functionalization of the *tert*-butyl group for further synthetic elaboration.

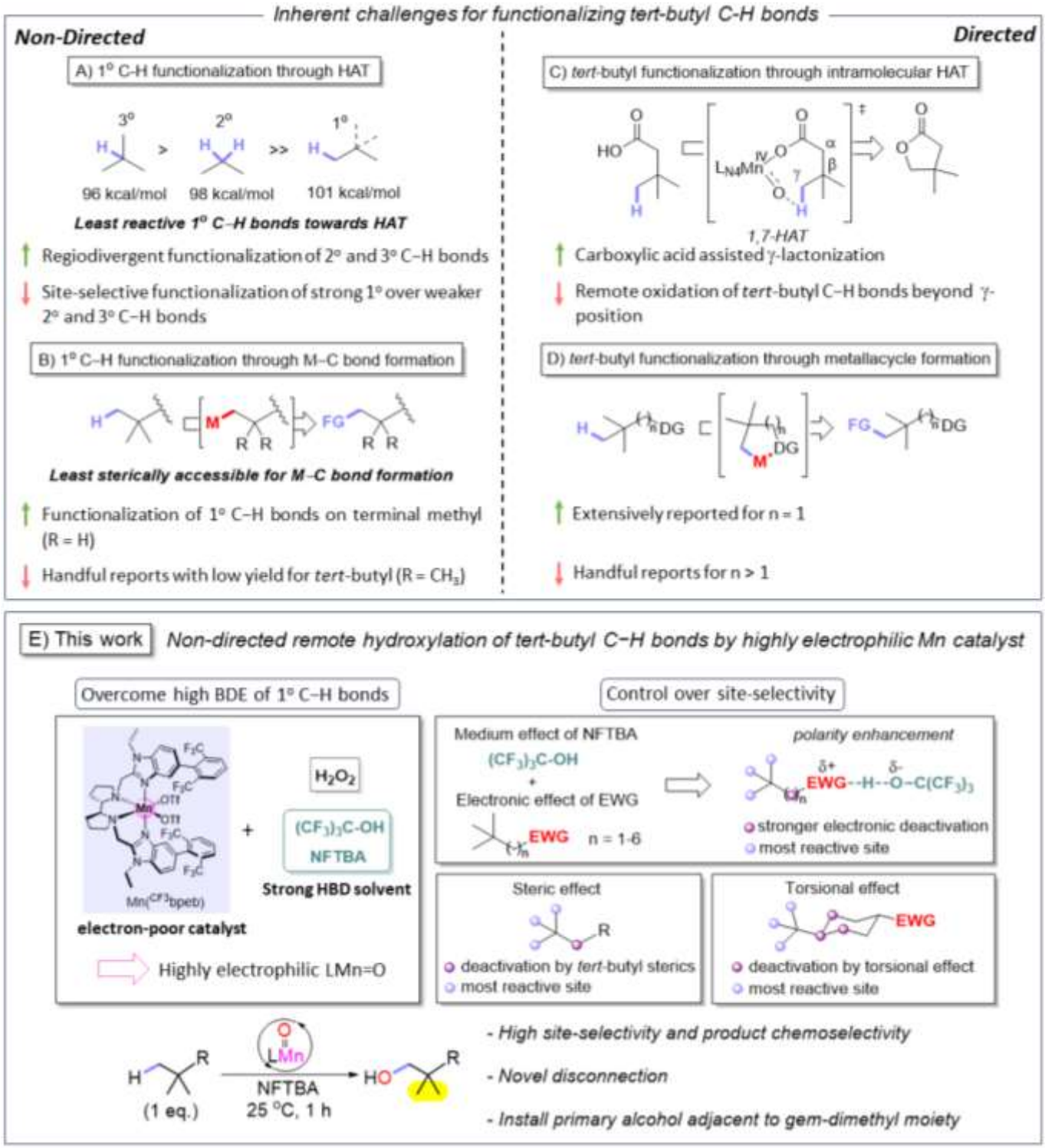

Scheme 1. Summary of the inherent challenges for functionalization of *tert*-butyl C−H bonds by state-of-the-art methodologies: (A) Non-directed HAT based functionalization. (B) Non-directed functionalization through M−C bond formation. (C) Carboxylic acid directed γ-lactonization through intramolecular HAT. (D) Directing group approach through metallacycle formation. (E) Summary of the main features of the present work to achieve non-directed remote hydroxylation.

Results and discussion

Reaction development on 2,2,3,3-tetramethylbutane (S1)

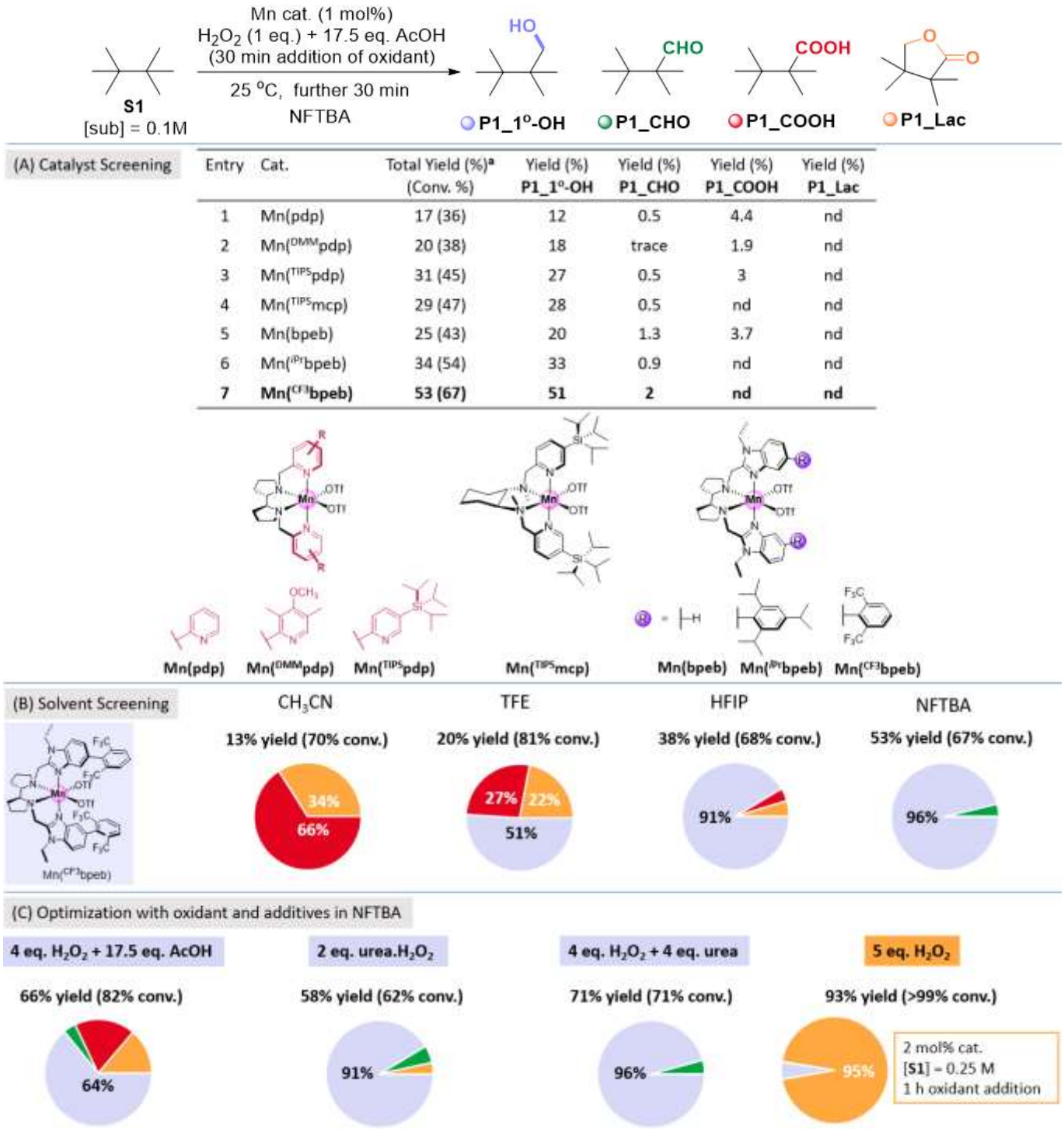

Entry	Cat.	Total Yield (%)[a] (Conv. %)	Yield (%) P1_1°-OH	Yield (%) P1_CHO	Yield (%) P1_COOH	Yield (%) P1_Lac
1	Mn(pdp)	17 (36)	12	0.5	4.4	nd
2	Mn(^{DMM}pdp)	20 (38)	18	trace	1.9	nd
3	Mn(^{TIPS}pdp)	31 (45)	27	0.5	3	nd
4	Mn(^{TIPS}mcp)	29 (47)	28	0.5	nd	nd
5	Mn(bpeb)	25 (43)	20	1.3	3.7	nd
6	Mn(^{iPr}bpeb)	34 (54)	33	0.9	nd	nd
7	**Mn(^{CF3}bpeb)**	**53 (67)**	**51**	**2**	**nd**	**nd**

Figure 1. Reaction development on **S1**: (A) Catalyst screening. (B) Solvent screening. (C) Optimization with oxidant and additives. [a]Initial conditions: substrate (0.1 M), Mn catalyst (1 mol%) and AcOH were dissolved in NFTBA; 1 eq. of H_2O_2 (0.35 M in NFTBA) was delivered over 30 min with a syringe pump followed by additional 30 min reaction time at 25 °C, unless otherwise indicated. Catalysts enantiomers were used interchangeably. Substrate conversion and product yields were determined by GC-FID with biphenyl as internal standard. The pie charts indicate product selectivity. Full reaction details are available in the SI, Tables S1-S6.

2,2,3,3-Tetramethylbutane, **S1** was chosen for reaction development. The oxidation of **S1** (0.1 M) was initially conducted using 1 eq. of H_2O_2 (0.35 M in NFTBA) delivered over 30 min by syringe pump to an open-to-air vial containing 17.5 eq. of AcOH and 1 mol% of the Mn catalyst in a NFTBA stirred solution

at 25 ºC for a total reaction time of 1 hour. A series of manganese catalysts bearing tetraazadentate ligands, containing pyridine or benzimidazole donors, were employed (**Figure 1A**). In all cases, the reaction delivered 2,2,3,3-tetramethylbutanol (**P1_1º-OH**) as the major product accompanied by minor amounts of 2,2,3,3-tetramethylbutanal (**P1_CHO**) and 2,2,3,3-tetramethylbutanoic acid (**P1_COOH**). In general, improved yields were obtained when employing sterically encumbered catalysts (compare entry 1 with entries 3 and 4, and entry 5 with entries 6 and 7). Notably, the catalyst bearing the ligand anchored with electron-withdrawing substituents, Mn(^{CF3}bpeb) gave the best performance delivering **P1_1º-OH** in 51% yield accompanied by a trace amount (2%) of **P1_CHO** as overoxidation product, achieving 96% product selectivity (entry 7). In sharp contrast, when the iron catalyst analogue Fe(^{CF3}bpeb) was employed, <1% of oxidation products were observed (see SI, Table S1). A progressive decrease in both product chemoselectivity and mass balance was observed with decreasing solvent HBD ability, i.e. going from NFTBA to 1,1,1,3,3,3-hexafluoro-2-propanol (HFIP), 2,2,2-trifluoroethanol (TFE) and CH_3CN (**Figure 1B**). Accordingly, the relative amount of the overoxidized carboxylic acid (**P1_COOH**) and γ-lactone (**P1_Lac**) products, that were not observed in NFTBA, are detected in trace amounts (<2 %) in HFIP, and become the exclusive products observed, albeit in low overall yield, in CH_3CN. These observations highlight the synergistic contribution of the electron-poor Mn(II) catalyst and solvent HBD ability in achieving the hydroxylation product **P1_1º-OH** in high yield and chemoselectivity. Presumably, the very strong HBD character of NFTBA plays a dual function: 1) it enhances the electrophilicity of the Mn-oxo catalyst through interaction with the ligand set; and 2) induces a polarity reversal effect in the first formed alcohol product, that prevents overoxidation[31,33].

Further optimization targeting the amount of oxidant, catalyst and carboxylic acid loading and substrate concentration did not improve the reaction outcome. (Table S3). However, overall yield, chemoselectivity and mass balance could be improved to 71%, 96% and >99%, respectively when replacing acetic acid by urea (4 eq.) (**Figure 1C**). These results point toward an important role played by urea in preventing overoxidation of **P1_1º-OH**[42]. In contrast, lactone **P1_Lac**, deriving from intramolecular lactonization in the overoxidized product **P1_COOH** was obtained in excellent yield (88%) and outstanding selectivity over **P1_1º-OH** (95%) in the absence of AcOH, employing higher H_2O_2 (5 eq.) and catalyst loadings (2 mol%), 0.25 M substrate concentration and a longer oxidant addition time (1 h). The reaction is particularly notable because it entails the one-pot consecutive and highly selective oxidation of two primary C−H bonds.

Effect of *tert*-butyl sterics on site-selectivity

We then explored the effect of *tert*-butyl sterics on the competition between primary and secondary C−H bond oxidation[4,7,43-45]. For this purpose, 2,2,4,4-tetramethylpentane (**S2**) and 2,2,5,5-tetramethylhexane (**S3**) were selected as substrates. Oxidation of both **S2** and **S3** exclusively delivered products deriving from primary C−H bond oxidation despite the presence of weaker and intrinsically more activated secondary C−H bonds (**Figure 2**). Reactions proceeded with excellent mass balance, delivering the primary alcohols deriving from *tert*-butyl C−H bond hydroxylation (**P2_1º-OH** and **P3_1º-OH**) in 60% and 53% yield, respectively, and ≥91% product chemoselectivity over overoxidized aldehyde and diol products. These observations clearly indicate that methylenic units adjacent to *tert*-butyl groups are effectively shielded by steric congestion that prevents their functionalization. The significance of the yields and chemoselectivities obtained in these reactions are best appreciated when compared with state-of-the-art literature. For instance, with **S2** both copper-mediated and metal-free C−H bond borylation has been reported using a 5 eq. substrate excess, yielding 84 and 40% of the primary borylated product, respectively, with 97% selectivity over the secondary ones[46,47].

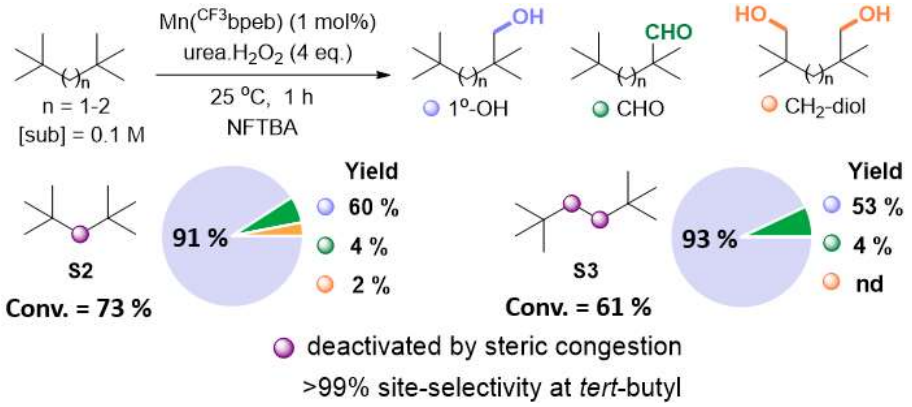

Figure 2. Effect of *tert*-butyl sterics on the oxidation of **S2** and **S3**. The pie charts indicate product selectivity while individual product yields are indicated by the small circles. Substrate conversion and product yields were determined by GC-FID with biphenyl as internal standard. Full reaction details are available in the SI, Table S7.

Remote selectivity induced by electronic effects of functional groups

Due to the electrophilic nature of metal-oxo species, it is well established that electron-withdrawing groups (EWGs) in the substrate can deactivate proximal C−H bonds toward HAT to these reagents by a polarity mismatching effect[12,48]. To systematically evaluate the impact of these groups on the oxidation of *tert*-butyl C−H bonds, 1-(2,2,3,3-tetramethyl)butylpivalate, acetate, pivalamide and acetamide (**S4-S7**, respectively) and 1-(2,2,4,4-tetramethyl)pentylacetate (**S8**) were used to examine the oxidation site-selectivity, and results compared with those obtained for **S1** and **S2**, respectively. Reactions were performed using 4 eq. of urea.H_2O_2 as oxidant (**Figure 3**). In all cases, predominant formation of the alcohol product deriving from hydroxylation at a remote primary C−H bond was observed in modest yield (16-29%) and very good product chemoselectivity (86-91%), while products resulting from oxidation at the methylenic site adjacent to the functional group were detected in only trace amounts (<1%). Of notice, product yields are greatly decreased when compared to the corresponding oxidations of **S1** and **S2**, reflecting electronic deactivation of the primary C−H bonds.

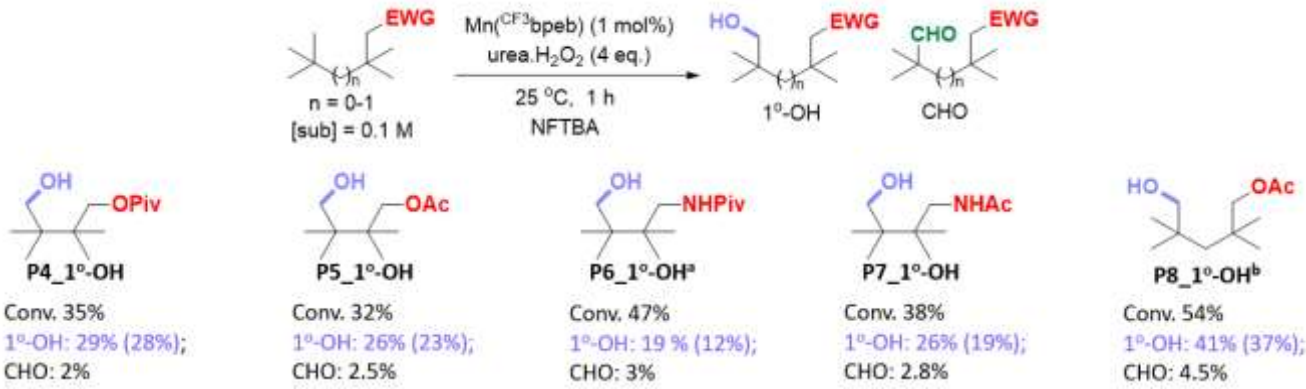

Figure 3. Effect of EWGs on the oxidation of **S4-S8**. Substrate conversion and product yields were determined by GC-FID with biphenyl as internal standard. Isolated yields are indicated in parentheses. [a]2 mol% cat. [b]>99% site-selectivity at *tert*-butyl C−H bonds. Full details on the reactions and associated product distributions are available in the SI, Tables S8-S17.

Along this line, a significant increase in yield was observed going from **S5** to **S8**, where OAc is moved one carbon away from the *tert*-butyl group, a behaviour that can be accounted for on the basis of a reduced electronic deactivation determined by the remote EWG. Notably, **P8_1°-OH** could be obtained in 41% yield along with 4.5% of the corresponding formyl derivative, showing that oxidation occurs with exquisite site-selectivity and compares positively with the 26% yield of **P5_1°-OH** obtained in the oxidation of **S5**.

Solvent induced polarity enhancement has been recently described as an effective strategy to enhance selectivity for oxidation at the most remote methylenic site of linear alkyl chains bearing terminal EWGs[49-51]. For instance, oxidation of 1-heptyl derivatives by Mn(^{TIPS}mcp) in NFTBA led to predominant functionalization (up to 88% site-selectivity) at the most remote (C6) methylenic site[51]. However, with 1-pentyl, 1-hexyl and 1-heptyl derivatives, the primary C−H bonds at the terminal methyl group were never oxidized. Replacing the terminal ethyl by a *tert*-butyl is envisaged as a strategy to invert the selectivity between primary and secondary C−H bonds because of the specific structural characteristics of the latter group. In first place, the steric hindrance exerted by the *tert*-butyl group prevents oxidation at the adjacent and most remote methylenic site, as seen in the oxidations of **S2**, **S3** and **S8**. As a result of the presence of a quaternary carbon, compared to the linear derivative, the first accessible methylenic site is now moved two positions closer to the deactivating EWG, further magnifying electronic differences between competing primary and secondary sites. Finally, a statistic factor plays moreover in favour of primary C−H bond oxidation because of the 9 equivalent *tert*-butyl C−H bonds.

To explore the limits of the selectivity toward primary sites determined by polarity enhancement, the substrate scope was expanded to a series of alkyl pivalates bearing a terminal *tert*-butyl group (substrates C*n*-OPiv, **S9-S14** in **Figure 4**; *n* = number of methylene spacers between *tert*-butyl and OPiv functionality), where competition for oxidation at remote methylenic sites is anticipated to increase with increasing distance between the *tert*-butyl and OPiv groups. When C1-OPiv (**S9**) was oxidized, >95% substrate was recovered without detection of oxidation products, in line with the strong electronic deactivation of all primary and secondary C−H bonds. A progressive increase in substrate conversion and oxidation yield was observed with increasing the number of methylene spacers from C2 to C6, accompanied however by a decrease in the primary site-selectivity ratio (1° s*r*; relative ratio of oxidation products derived from *tert*-butyl C−H over other C−H bonds). A >9 1° *sr* is maintained for C2-OPiv (**S10**), C3-OPiv (**S11**) and C4-OPiv (**S12**). A progressive decrease in 1° *sr* was observed with increasing number of methylenic spacers, 1° *sr* = 3.9 and 1.3, respectively for C5-OPiv (**S13**) and C6-OPiv (**S14**), reflecting the increased competition for oxidation at secondary C−H bonds. Notably, 1°-OH remain the predominant products from C2-OPiv to C6-OPiv and in all cases the corresponding overoxidation products account for <4%. Product yields also consistently respond to the proximity of the reactive site to the EWG. A progressive increase in yield of the 1°-OH product from C2-OPiv (13%) to C4-OPiv (43%) was observed, which represents the highest 1°-OH yield within the C*n*-OPiv series (see SI, Table S27 for details about the oxidation C3-OPiv to C5-OPiv in different solvent media).

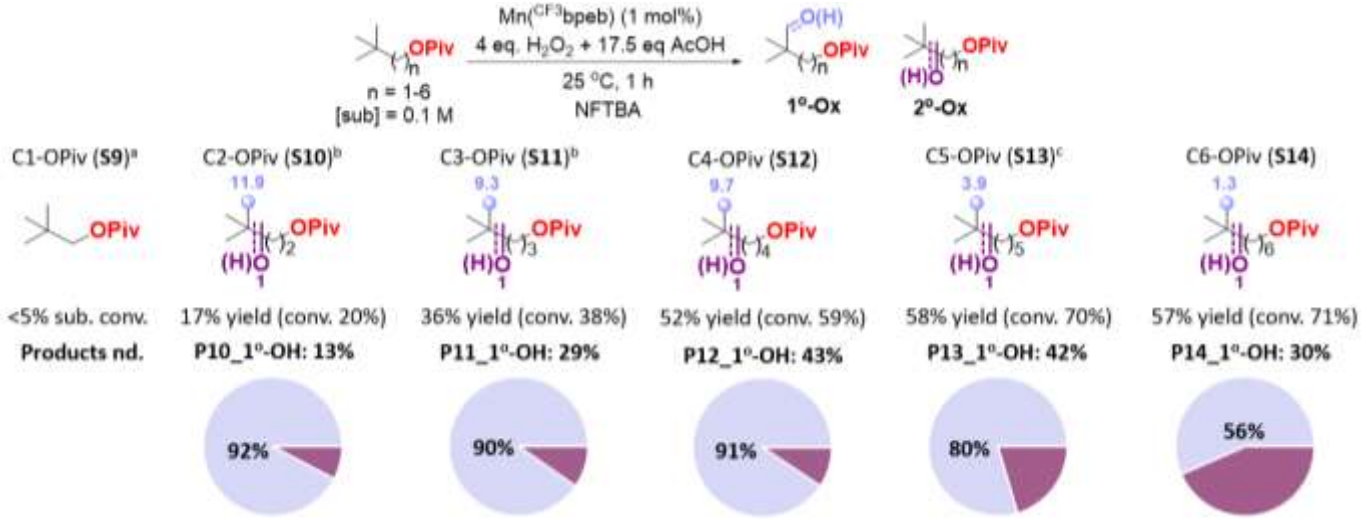

Figure 4. C*n*-OPiv substrates from C1 to C6 were selected to investigate the distal electronic effect on oxidation of *tert*-butyl C−H bonds. Substrate conversion and product distribution were determined by GC-FID with biphenyl as internal standard. [a]5 mol% of catalyst. [b]2 mol% of catalyst. [c]1,3,5-trimethoxybenzene was used as internal standard for GC-FID. Full reaction details are available in the SI, Tables S18-S29.

Building on these results, the substrate scope was further expanded to other EWGs as hydrogen bond acceptors (HBA). The catalytic oxidation of substrates C*n*-EWG in NFTBA are presented in **Table 1**. The data shows that the 1° *sr* is influenced by the nature of the EWG. Replacing OPiv by more electron withdrawing 4-nitrobenzoate (4-NBz), 3,5-dinitrobenzoate (3,5-DNBz) or CN, the 1° *sr* increases substantially. For instance, the oxidation of C4-3,5-DNBz (**S15**) and C4-CN (**S21**) proceeded with two of the highest 1° *sr* (14.8 and 13.8 respectively) among the C*n*-EWG substrates. This improvement is even more significant for the C5 and C6 substrates. Notably, the 1° *sr* increased from 1.3 to 2.7 going from C6-OPiv (**S14**) to C6-3,5-DNBz (**S17**), delivering **P17_1°-OH** in a synthetically valuable 34% yield.

With methyl alkanoate esters (C*n*-CO_2CH_3, **S23**-**S26**), results were comparable with those obtained for the corresponding C*n*-OPiv substrates, both in in terms of 1°-OH yield and 1° *sr*. Primary C−H bond oxidation in C5-CO_2CH_3 (**S26**) proceeded with 1° *sr* = 3.4. We note that this selectivity for the primary site exceeds those reported for remote secondary C−H bond oxidation of methylhexanoate catalyzed by $[Fe(pdp)]^{2+}$ in CH_3CN which delivered ketone products derived from oxidation at the most remote methylenic C4 over C3 in a 2.3:1 selectivity[7]. Considering that the primary C−H bonds in **S26** are seven carbons away from the EWG, the site-selectivity obtained in the oxidation of this substrate is truly exceptional.

On the contrary, the 1° *sr* drops in the oxidation of amide derivatives. The difference is apparent by directly comparing results from the oxidation of C*n*-OPiv **S11**-**S13** with the corresponding C*n*-NHPiv substrates **S27**-**S29**. The decrease in 1° *sr* for the latter series could be restored by changing to a more electron withdrawing group such as 4-nitrosulfonamide (NHNs) for **S30** and **S31**. Comparable 1° *sr* values were observed for C6-NHNs (**S31**) and C6-3,5-DNBz (**S17**).

The reach of this selectivity frame is well exemplified in the oxidation of 1-(2,5,5-trimethyl)hexyl acetate (**S32**), that contains both primary, secondary and tertiary C−H bonds. Oxidation was selective for the remote primary C−H bonds with a 1° *sr* of 7.3 and **P32_1°-OH** obtained in 40% yield as predominant product. On the other hand, the oxidation of 5,5-dimethyl-1-hexanol C4-OH (**S33**) bearing a primary alcohol functionality, illustrates the extent and limitation of the deactivating role of NFTBA in functional groups a priori sensitive to oxidation. Hydroxylation of the *tert*-butyl group is favoured over α–C−H oxidation, with a 1° *sr* of 1.6, delivering the diol as the major product (21% yield).

Table 1. Oxidation of C*n*-EWG substrates.

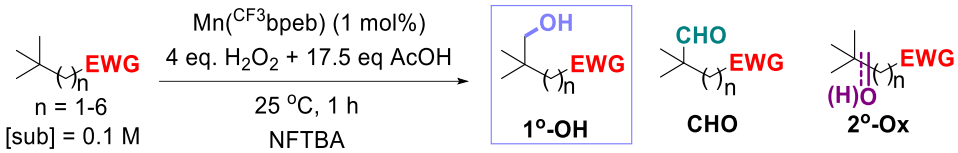

		Sub. Conv. (%)[a]	Total Yield (%)[a]	1°-OH yield (%)[a] (Isolated % Yield)	1° *sr*[a]
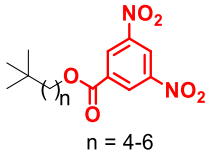 n = 4-6	**S15** (C4)	45	37	31 (25)	14.8
	S16 (C5)	50	40	32 (28)	6.8
	S17 (C6)	64	52	34 (30)	2.7
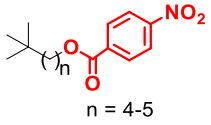 n = 4-5	**S18** (C4)	38	31	26 (22)	11.4
	S19 (C5)	56	42	32 (26)	5.1
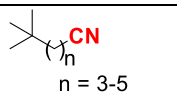 n = 3-5	**S20**(C3)[c]	31	29	22 (18)	9.8
	S21 (C4)[b]	50	39	33 (31)	13.8
	S22 (C5)[b]	64	48	37 (30)	5.4
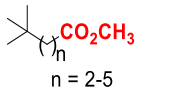 n = 2-5	**S23** (C2)[b]	13	11	7 (8)[b,c]	10.1
	S24 (C3)[b,c]	54	43	35 (28)	9.7
	S25 (C4)[b]	64	46	38 (32)	9.6
	S26 (C5)[b]	70	54	39 (34)	3.5
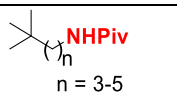 n = 3-5	**S27** (C3)	47	36	27 (24)	4.8
	S28 (C4)[b]	64	42	28 (20)	2.8
	S29 (C5)[b]	79	58	36 (26)	2.2
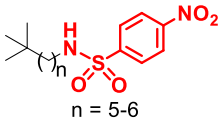 n = 5-6	**S30** (C5)	49	35	25 (22)	4.5
	S31 (C6)	69	42	26 (24)	2.5
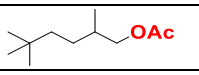	**S32**	57	50	40 (37)	7.3
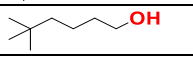	**S33**[c]	49	38	21 (12)	1.6

[a]The substrate conversion, product yield and 1° *sr* were determined by GC-FID with biphenyl as internal standard. Isolated yields are indicated in parentheses. [b]2 mol% cat. [c]4 eq. urea.H_2O_2 without AcOH. Full reaction details are available in the SI, Tables S30-S66.

Torsional effects on the oxidation of 4-*tert*-butylcyclohexane derivatives

Moving to cyclohexane derivatives, torsional effects were explored as directing tools for *tert*-butyl group oxidation[52,53]. Starting with *cis* and *trans* methyl 4-*tert*-butylcyclohexanecarboxylate (*cis*: **S34**; *trans*: **S35**), oxidation in NFTBA delivered different selectivity profiles (**Figure 5**). Oxidation of the *cis*-diastereoisomer (**S34**), generated a mixture of cyclohexane oxidation products in overall 56% yield, including 4% of *tert*-butylcyclohexanone as C1 oxidative cleavage product (see Figure S2 in the SI for full details of the product distribution). **P34_1°-OH**, deriving from *tert*-butyl C−H bond hydroxylation, was formed as a minor product in 13% yield. Instead, oxidation of the *trans* diastereoisomer occurred with high 1° *sr* (8.9), delivering **P35_1°-OH** in 48% yield. The remarkable site-selective *tert*-butyl C−H bond hydroxylation in **S35** can be explained in terms of an effective deactivation of the cyclohexane C−H bonds dictated by electronic, torsional and steric effects, thus enforcing *tert*-butyl as the preferential site for oxidation. Torsional effects account, in addition to electronic ones, for deactivation of the C_2−H and axial C_1−H bonds in **S35** because HAT from these sites would result in planarization of the incipient carbon radical forcing unfavourable eclipsed conformations[52,54]. The same rationale associated to a greater extent of such deactivation imposed by the bulkier *tert*-butyl group holds for the C_3−H and C_4−H bonds.

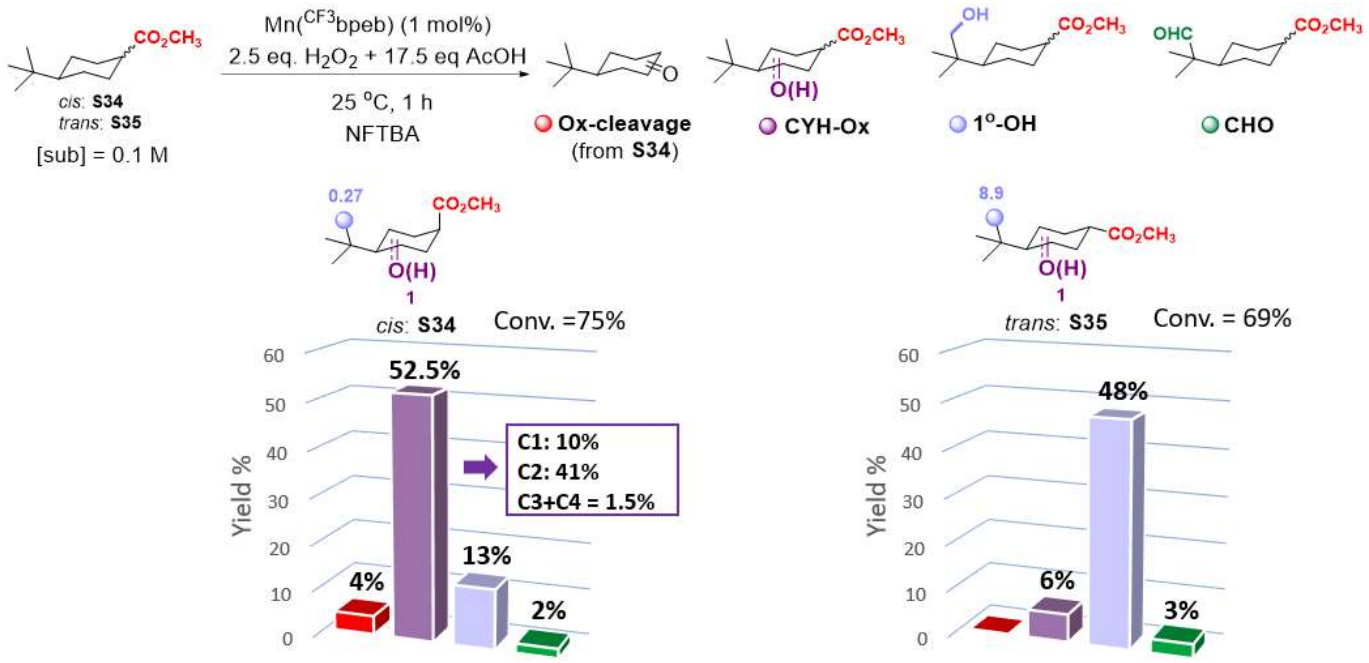

Figure 5. Oxidation of *cis* and *trans* methyl 4-*tert*-butylcyclohexanecarboxylates (**S34** and **S35**). Substrate conversion and product yields on the bar chart were determined by GC-FID with biphenyl as internal standard.

Based on this finding, the oxidation of a series of *trans* 1-EWG-4-*tert*-butylcyclohexanes, **S36-S46** was explored, aiming at selectively hydroxylating the *tert*-butyl C−H bonds (**Figure 6**). Encouragingly, oxidation of these substrates consistently resulted in remarkable site- and chemoselectivities, with the corresponding primary alcohol derived from *tert*-butyl C-H bond hydroxylation observed as the major product in satisfactory yield. Cyclohexane derivatives **S35-S39** feature the same number of carbon atoms between the *tert*-butyl and the EWG as their acyclic C4-EWG analogues, and were all hydroxylated at the primary C−H bonds with high site-selectivity (≥90%). Of notice, for substrates that contain bulky EWGs (**S36-S39**), significant improvements in 1° *sr* were observed when compared to the corresponding C4-EWG substrates. For example, 1° *sr* increases substantially from 2.8 in C4-NHPiv (**S28**) to an excellent 19.8 in **S37** characterized by the presence of the same group. This drastic enhancement can be explained in terms of the steric shielding and torsional effect exerted by the bulky EWG on the C_2−H bonds. Within these substrates, the highest selectivity for primary C−H oxidation was observed for **S39** (1° *sr* 28.1) which bears the bulky and strongly EW 3,5-DNBz. For 4-*tert*-butyl cyclohexanone (**S40**), the presence of the carbonyl group in the cyclohexane ring exerts an additional electronic deactivation which translates into a modest yield of **P40_1°-OH** (25%). However, a high 1° *sr* (13.1) was still achieved.

Interestingly, the high 1° *sr* observed in the oxidation of these substrates is maintained when the EWGs are moved one methylenic unit away from the cyclohexane scaffold (**S41-S46)**, and remains comparatively higher than the selectivities observed for acyclic C5-EWG substrate analogues. Of notice, because of the improvement in 1° *sr*, with **S42**, bearing the CH_2OPiv group at C1, a notable 54% yield of the 1°-OH product **P42_1°-OH** was obtained. As previously noticed, simple amides exert a weaker deactivation. Thus, oxidation of amide containing derivatives **S45** and **S46** led to significantly smaller 1° *sr* values (2.5 and 4.1, respectively). Moreover, the aldehyde product (8%) resulting from oxidation at the methylenic spacer was observed in the oxidation of **S45**.

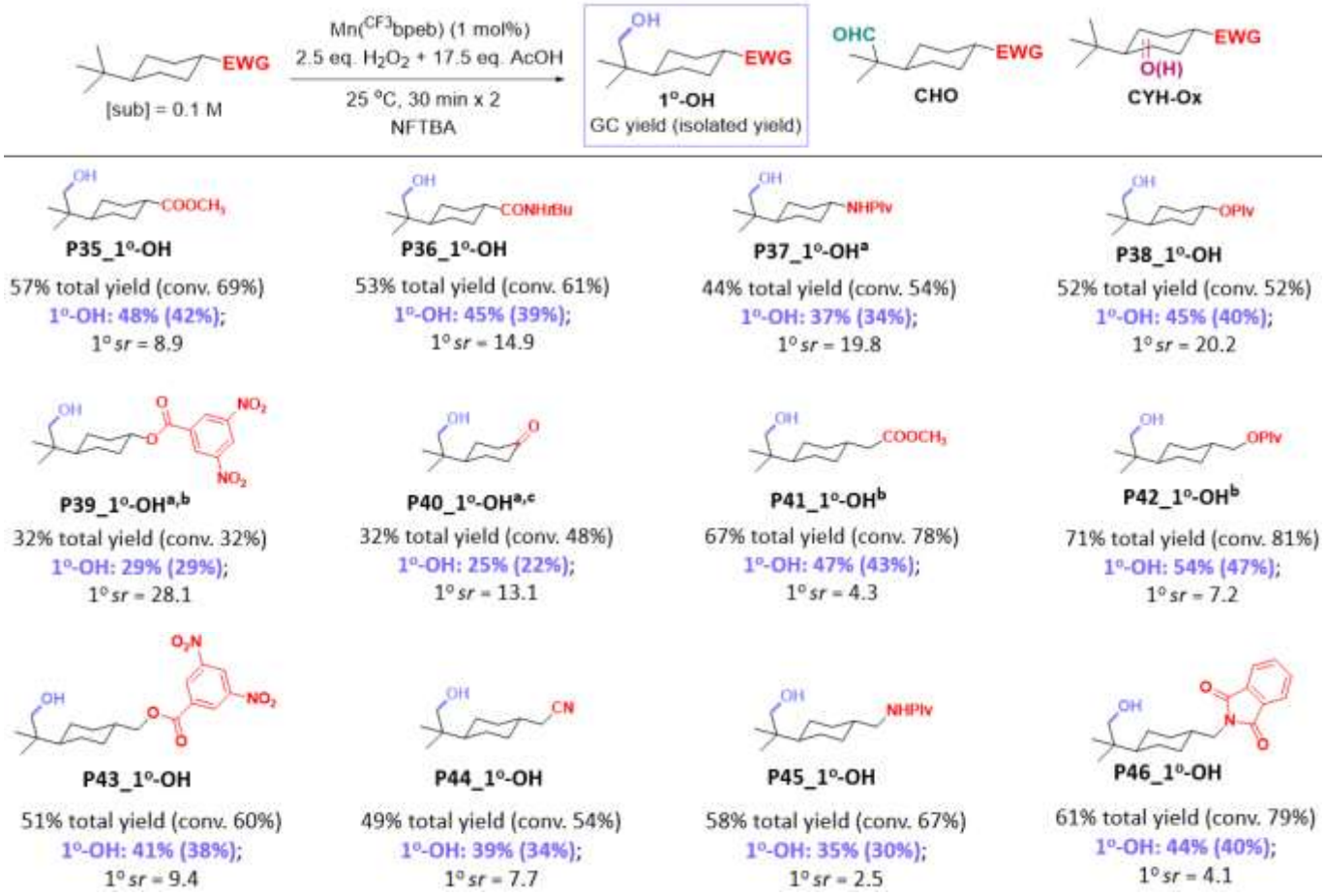

Figure 6. Oxidation of 1-EWG-4-*tert*-butylcyclohexanes. Substrate conversion, product yield and 1^o *sr* were determined by GC-FID with biphenyl as internal standard. Isolated yields are indicated in parentheses. [a]2 mol% cat. [b]4 eq. H_2O_2. [c]4 eq. urea.H_2O_2 without AcOH. Full reaction details are available in the SI, Tables S67-S92.

Late-stage hydroxylation of *tert*-butyl containing pharmaceuticals

With a general understanding of the selectivity factors in hand, a valuable guideline for selective *tert*-butyl hydroxylation in complex molecular settings was established. Consequently, the oxidation of complex molecules of pharmaceutical interest containing a *tert*-butyl group (**Figure 7**) was explored. Capecitabine is an approved anticancer medication that contains a pentyl carbamate. Oxidation of its 1-(5,5-dimethylhexyl) carbamate derivative (**S47**) led to a satisfactory 28% isolated yield of **P47_1°-OH** and 39% recovered starting material (rsm). We reasoned that the presence of the 1,2-diol unit on the cyclic ether could potentially inhibit the catalyst through chelation of the metal and was thus protected by acetylation (**S48**). With this protection, the corresponding product **P48_1°-OH** was obtained in a notable 41% isolated yield accompanied by 51% rsm, displaying an excellent mass balance. The 1°-OH products were also obtained from oxidation of the 1-(5,5-dimethylhexyl) acetate derivative of Ciprofibrate (**S49**) and 1-(5,5-dimethylhexyl) carbamate derivative of Efavirenz derivatives (**S50**) in 33% and 31% isolated yield, respectively. We further examined the oxidation of Buparvaquone (**S51**) which is an antiprotozoal drug that contains a *trans* 4-*tert*-butylcyclohexane moiety. Although the hydroxylnaphthoquinone unit is highly oxidation and pH sensitive, which in principle is not favourable in our acidic catalytic condition, 18% of the corresponding hydroxylation product **P51_1°-OH** could still be isolated. The yield could be greatly improved if the enol functionality was protected by acetylation (**S52**), leading to **P52_1°-OH** in 43% isolated yield. This system resembles the t*rans* 4-*tert*-butylcyclohexane derivatives displayed in **Figure 6** where remote *tert*-butyl oxidation was dictated by the combination of torsional and steric effects. In addition, it must be further highlighted that rsm accounted for most of the mass balance of the reactions, further crediting the synthetic utility of these reactions. Lastly, we examined the oxidation of 4-(*tert*-

butyl)piperidine derivative (**S53**) as such heterocyclic systems are prevalent throughout FDA approved drugs[55]. We could obtain **P53_1°-OH** in 19% isolated yield which represents a significant improvement when compared to the previously reported platinum-catalyzed C−H oxidation of 4-(*tert*-butyl)piperidine (employed in a 5-fold excess) that yielded <5% of the *tert*-butyl C−H oxidation product[21].

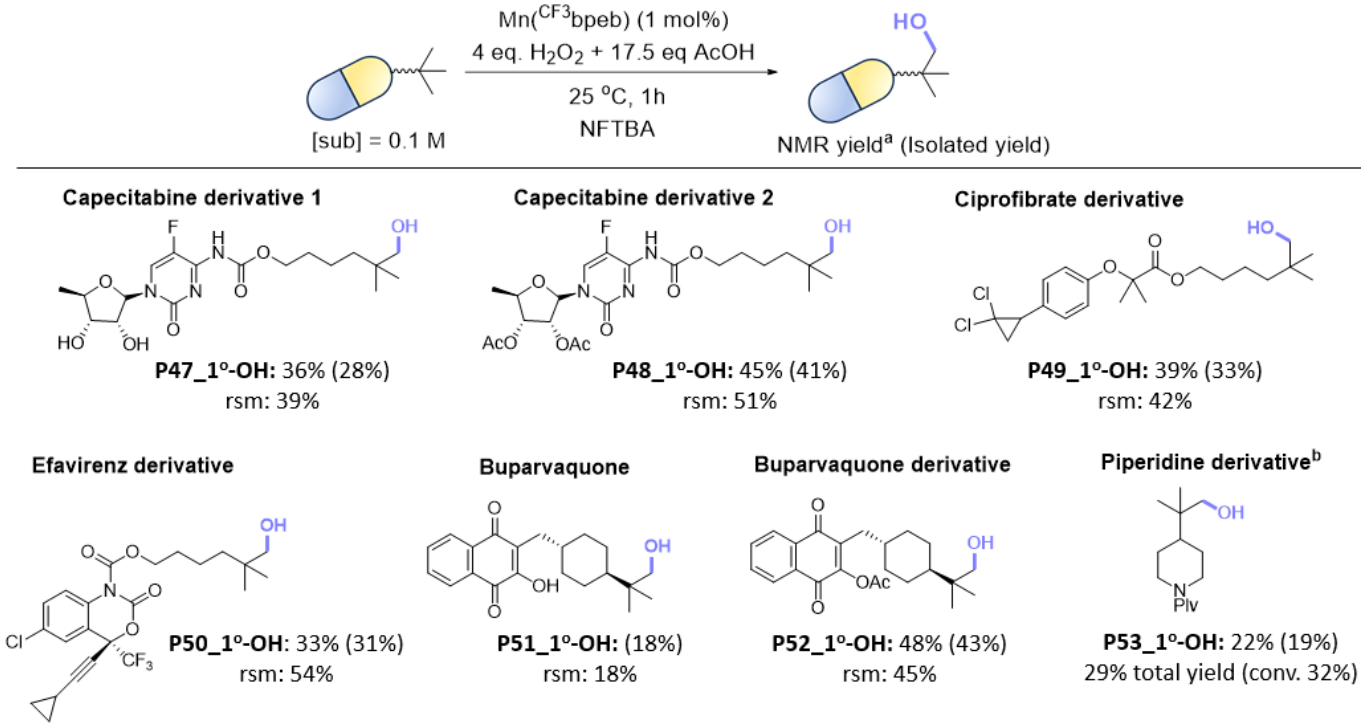

Figure 7. Late-stage hydroxylation of *tert*-butyl containing pharmaceuticals. [a]1,3,5-trimethoxybenzene as internal standard. [b]Substrate conversion and product yield were determined by GC-FID with biphenyl as internal standard.

Conclusion

This work pioneers site-selective non-directed hydroxylation of remote primary C−H bonds in *tert*-butyl groups employing hydrogen peroxide and the highly electrophilic Mn(CF3bpeb) catalyst in NFTBA. The strong HBD ability of NFTBA enhances the electrophilicity of the Mn-oxo overcoming the high BDE of *tert*-butyl C−H bonds. In addition, both polarity enhancement and polarity reversal effects exerted by this solvent enable highly site-selective and product chemoselective hydroxylation of primary C−H bonds, allowing isolation in synthetically amenable yields of the 1°-OH products that can be diversely elaborated by conventional methods[56]. The synergistic interplay of steric, electronic, medium and torsional effects operating in the HAT step, enforces selectivity for oxidation of *tert*-butyl C−H bonds over weaker secondary and tertiary ones. Capitalizing on high-valent metal-oxo catalysis, this understanding provides valuable guidelines for expanding the horizon of non-directed C(sp^3)−H oxidation from secondary and tertiary C−H bonds towards the uncharted domain of primary ones. These guidelines serve as the cornerstone for late-stage functionalization of *tert*-butyl containing molecules of pharmaceutical interest.

Remarkably, the selective hydroxylation of *tert*-butyl groups emerges as more than an atomic transformation from C−H to C−O, offering an innovative approach for molecular disconnection. It installs the chemically versatile primary alcohol functionality adjacent to a *gem*-dimethyl moiety, uncovering *tert*-butyl as an unprecedently recognized functional group more than just a sterically encumbered structural motif.

References

1. Chen, M. S. & White, M. C. A predictably selective aliphatic C−H oxidation reaction for complex molecule synthesis. *Science* **318**, 783-787 (2007).

2. Genovino, J., Sames, D., Hamann, L. G. & Touré, B. B. Accessing drug metabolites via transition-metal catalyzed C−H oxidation: The liver as synthetic inspiration. *Angew. Chem. Int. Ed.* **55**, 14218-14238 (2016).
3. White, M. C. & Zhao, J. Aliphatic C−H oxidations for late-stage functionalization. *J. Am. Chem. Soc.* **140**, 13988-14009 (2018).
4. Milan, M., Salamone, M., Costas, M. & Bietti, M. The quest for selectivity in hydrogen atom transfer based aliphatic C−H bond oxygenation. *Acc. Chem. Res.* **51**, 1984-1995 (2018).
5. Chakrabarty, S., Wang, Y., Perkins, J. C. & Narayan, A. R. H. Scalable biocatalytic C−H oxyfunctionalization reactions. *Chem. Soc. Rev.* **49**, 8137-8155 (2020).
6. Guillemard, L., Kaplaneris, N., Ackermann, L. & Johansson, M. J. Late-stage C−H functionalization offers new opportunities in drug discovery. *Nat. Rev. Chem.* **5**, 522-545 (2021).
7. Chen, M. S. & White, M. C. Combined effects on selectivity in Fe-catalyzed methylene oxidation. *Science* **327**, 566-571 (2010).
8. Newhouse, T. & Baran, P. S. If C−H bonds could talk: selective C−H bond oxidation. *Angew. Chem. Int. Ed.* **50**, 3362-3374 (2011).
9. Davies, H. M. L. & Liao, K. Dirhodium tetracarboxylates as catalysts for selective intermolecular C−H functionalization. *Nat. Rev. Chem.* **3**, 347-360 (2019).
10. Xia, G., Weng, J., Liu, L., Verma, P., Li, Z. & Yu, J.-Q. Reversing conventional site-selectivity in C(sp^3)−H bond activation. *Nat. Chem.* **11**, 571-577 (2019).
11. Costas, M. Site and enantioselective aliphatic C−H oxidation with bioinspired chiral complexes. *Chem. Rec.* **20**, 4000-4014 (2021).
12. Ruffoni, A., Mykura, R. C., Bietti, M. & Leonori, D. The interplay of polar effects in controlling the selectivity of radical reactions. *Nat. Synth.* **1**, 682-695 (2022).
13. Lu, Z., Ju, M., Wang, Y., Meinhardt, J. M., Alvarado, J. I. M., Villemure, E., Terrett, J. A. & Lin, S. Regioselective aliphatic C−H functionalization using frustrated radical pairs. *Nature* **619**, 514-521 (2023).
14. Mayer, M. M. Understanding hydrogen atom transfer: from bond strengths to Marcus theory. *Acc. Chem. Res.* **44**, 36-46 (2011).
15. Hartwig, J. F. & Larsen, M. A. Undirected, homogeneous C−H bond functionalization: challenges and opportunities. *ACS Cent. Sci.* **2**, 281-292 (2016).
16. He, J., Wasa, M., Chan, K. S. L., Shao, Q. & Yu, J.-Q. Palladium-catalyzed transformations of alkyl C−H bonds. *Chem. Rev.* **117**, 8754-8786 (2016).
17. Xue, X.-S., Ji, P., Zhou, B. & Cheng, J.-P. The essential role of bond energetics in C−H activation/functionalization. *Chem. Rev.* **117**, 8622-8648 (2017).
18. Chu, J. C. K. & Rovis, T. Complementary strategies for directed C(sp^3)−H functionalization: A comparison of transition-metal-catalyzed activation, hydrogen atom transfer, and carbene/nitrene transfer. *Angew. Chem. Int. Ed.* **57**, 62-101 (2018).
19. Bisel, P., Al-Momani, L. & Müller, M. The *tert*-butyl group in chemistry and biology. *Org. Bimol. Chem.* **6**, 2655-2665 (2008).
20. Cook, B. R., Reinert, T. J. & Suslick, K. S. Shape selective alkane hydroxylation by metalloporphyrin catalysis. *J. Am. Chem. Soc.* **108**, 7281-7286 (1986).
21. Lee, M. & Sanford, M. S. Platinum-catalyzed, terminal-selective C(sp^3)−H oxidation of aliphatic amines. *J. Am. Chem. Soc.* **137**, 12796-12799 (2015).
22. Juliá-Hernández, F., Moragas, T., Cornella, J. & Martin, R. Remote carboxylation of halogenated aliphatic hydrocarbons with carbon dioxide. *Nature* **545**, 84-89 (2017).
23. Sommer, H., Juliá-Hernández, F., Martin, R. & Marek, I. Walking metals for remote functionalization. *ACS Cent. Sci.* **4**, 153-165 (2018).
24. Li, X., Yang, X., Chen, P. & Liu, G. Palladium-catalyzed remote hydro-oxygenation of internal alkenes: an efficient access to primary alcohols. *J. Am. Chem. Soc.* **144**, 22877-22883 (2022).

25. Lepri, S., Goracci, L., Valeri, A. & Cruciani, G. Metabolism study and biological evaluation of bosentan derivatives. *Eur. J. Med. Chem.* **121**, 658-670 (2016).
26. Zwick, III, C. R. & Renata, Hans. Overview of amino acid modification by iron- and α-ketoglutarate-dependent enzymes. **13**, 4853-4865 (2023).
27. Ottenbacher, R. V., Talsi, E. P. & Bryliakov, K. P. Chiral manganese aminopyridine complexes: the versatile catalysts of chemo- and stereoselective oxidations with H_2O_2. *Chem. Rec.* **18**, 78-90 (2018).
28. Sun, W. & Sun, Q. Bioinspired manganese and iron complexes for enantioselective oxidation reactions: ligand design, catalytic activity, and beyond. *Acc. Chem. Res.* **52**, 2370-2381 (2019).
29. Vicens, L., Olivo, G. & Costas, M. Rational design of bioinspired catalysts for selective oxidations. *ACS Catal.* **10**, 8611-8631 (2020).
30. Chen, J., Jiang, Z., Fukuzumi, S., Nam, W & Wang, B. Artificial nonheme iron and manganese oxygenases for enantioselective olefin epoxidation and alkane hydroxylation reactions. *Coord. Chem. Rev.* **421**, No. 213443 (2020).
31. Dantignana, V., Milan, M., Cussó, O., Company, A., Bietti, M., Costas, M. Chemoselective aliphatic C−H bond oxidation enabled by polarity reversal. *ACS Cent. Sci.* **3**, 1350-1358 (2017).
32. Gaster, E., Kozuch, S. & Pappo, D. Selective aerobic oxidation of methylarenes to benzaldehydes catalyzed by *N*-hydroxyphthalimide and cobalt(II) acetate in hexafluoropropan-2-ol. *Angew. Chem. Int. Ed.* **56**, 5912-5915 (2017).
33. Bietti, M. Activation and deactivation strategies promoted by medium effects for selective aliphatic C−H bond functionalization. *Angew. Chem. Int. Ed.* **57**, 16618-16637 (2018).
34. Borrell, M., Gil-Caballero, S., Bietti, M. & Costas, M. Site-selective and product chemoselective aliphatic C−H bond hydroxylation of polyhydroxylated substrates. *ACS Catal.* **10**, 4702-4709 (2020).
35. Call, A., Cianfanelli, M., Besalú-Sala, P., Olivo, G., Palone, A., Vicens, L., Ribas, X., Luis, J. M., Bietti, M. & Costas, M. Carboxylic acid directed γ-Lactonization of unactivated primary C−H bonds catalyzed by manganese complexes: Application to selective natural product diversification. *J. Am. Chem. Soc.* **144**, 19542-19558. (2022).
36. Call, A., Capocasa, G., Palone, A., Vicens, L., Aparicio, E., Afailal, N. C., Siakavaras, N., Saló, E. L., Bietti, M. & Costas, M. Highly enantioselective catalytic lactonization at nonactivated primary and secondary γ- C−H bonds. *J. Am. Chem. Soc.* **145**, 18094-18103 (2023).
37. Morimoto, Y., Shimaoka, Y., Ishimizu, Y., Fujii, H. & Itoh, S. Direct observation of primary C−H bond oxidation by an oxido-iron(IV) porphyrin π-radical cation complex in a fluorinated carbon solvent. *Angew. Chem. Int. Ed.* **58** 10863-10866 (2019).
38. Dantignana, V., Company, A. & Costas, M. Catalytic oxidation of primary C−H bonds in alkanes with bioinspired catalyst. *Chimia* **74**, 470-477 (2020).
39. Morimoto, Y., Hanada, S., Kamada, R., Fukatsu, A., Sugimoto, H. & Itoh, S. Hydroxylation of unactivated C(sp^3)−H bonds with *m*-chloroperbenzoic acid catalyzed by an iron(III) complex supported by a trianionic planar tetradentate ligand. *Inorg. Chem.* **60**, 7641-7649 (2021).
40. Cook, S. A. & Borovik, A. S. Molecular designs for controlling the local environments around metal ions. *Acc. Chem. Res.* **48**, 2407-2414 (2015).
41. Liu, Y. & Lau, T.-C. Activation of metal oxo and nitrido complexes by Lewis acids. *J. Am. Chem. Soc.* **141**, 3755-3766 (2019).
42. Hahn, P. L., Lowe, J. M., Xu, Y., Burns, K. L. and Hilinski, M. K. Amine organocatalysis of remote, chemoselective C(sp^3)−H hydroxylation. *ACS Catal.* **12**, 4302-4309 (2022).
43. Moteki, S. A., Usui, A., Zhang, T., Alvarado, C. R. S. & Maruoka, K. Site-selective oxidation of unactivated C_{sp3}−H bonds with hypervalent iodine(III) reagents. *Angew. Chem. Int. Ed.* **52**, 8657-8660 (2013).
44. Milan, M., Bietti, M. & Costas, M. Highly enantioselective oxidation of nonactivated aliphatic C−H bonds with hydrogen peroxide catalyzed by manganese complexes. *ACS Cent. Sci.* **3** 196-204 (2017).

45. Ravelli, D., Fagnoni, M., Fukuyama, T., Nishikawa, T. & Ryu, I. Site-selective C−H functionalization by decatungstate anion photocatalysis: synergistic control by polar and steric effects expands the reaction scope. *ACS Catal.* **8** 701-713 (2017).
46. Shu, C., Noble, A. & Aggarwal, V. K. Metal-free photoinduced C(sp^3)−H borylation of alkanes. *Nature* **586**, 714-720 (2020).
47. Sang, R., Han, W., Zhang, H., Saunders, C. M., Noble, A. & Aggarwal, V. K. Copper mediated dehydrogenative C(sp^3)−H borylation of alkanes. *J. Am. Chem. Soc.* **145**, 15207-15217 (2023).
48. Galeotti, M., Salamone, M. & Bietti, M. Electronic control over site-selectivity in hydrogen atom transfer (HAT) based C(sp^3)−H functionalization promoted by electrophilic reagents. *Chem. Soc. Rev.* **51**, 2171-2223 (2022).
49. Griffin, J. D., Vogt, D. B., DuBois, J. & Sigman, M. S. Mechanistic guidance leads to enhanced site-selectivity in C−H oxidation reactions catalyzed by ruthenium bis(bipyridine) complexes. *ACS Catal.* **11**, 10479-10486 (2021).
50. Chen, J., Song, W., Yao, J., Wu, Z., Lee, Y.-M., Wang, Y., Nam, W. & Wang, B. Hydrogen-bonding assisted and nonheme manganese-catalyzed remote hydroxylation of C−H bonds in nitrogen-containing molecules. *J. Am. Chem. Soc.* **145**, 5456-5466 (2023).
51. Sisti, S., Galeotti, M., Scarchilli, F., Salamone, M., Costas, M. & Bietti, M. Highly selective C(sp^3)−H bond oxygenation at remote methylenic sites enabled by polarity enhancement. *J. Am. Chem. Soc.* **145** 22086-22096 (2023).
52. Milan, M., Bietti, M. & Costas, M. Aliphatic C−H bond oxidation with hydrogen peroxide catalyzed by manganese complexes: directing selectivity through torsional effect. *Org. Lett.* **20**, 2720-2723 (2018).
53. Martin, T., Galeotti, M., Salamone, M., Liu, F., Yu, Y., Duan, M., Houk, K. N. & Bietti, M. Deciphering reactivity and selectivity patterns in aliphatic C−H bond oxygenation of cyclopentane and cyclohexane derivatives. *J. Org. Chem.* **86**, 9925-9937 (2021).
54. Salamone, M., Ortega, V. B. & Bietti, M. Enhanced reactivity in hydrogen atom transfer from tertiary sites of cyclohexanes and decalins via strain release: equatorial C−H activation vs axial C−H deactivation. *J. Org. Chem.* **80**, 4710-4715 (2015).
55. Vitaku, E., T. Smith, D. & Njardarson, J. T. Analysis of the structural diversity, substitution patterns, and frequency of nitrogen heterocycles among U.S. FDA approved pharmaceuticals. *J. Med. Chem.* **57**, 10257-10274 (2014).
56. Liu, X., Rong, X., Liu, S., Lan, Y. & Liu, Q. Cobalt catalyzed desymmetric isomerization of exocyclic olefins. *J. Am. Chem. Soc.* **143**, 20633-20639 (2021).

Acknowledgments: Economic support from European Research Council, (AdvG 883922 to MC.) Spain Ministry of Science, (MINECO, PID2021-129036NB-I00 to MC). Generalitat de Catalunya, (ICREA Academia to MC, 2021 SGR 00475).We acknowledge STR of UdG for experimental support.

Author contributions:
S.-C.C. initiated the project, designed the substrate scope, and performed the experimental works. A.P. developed the catalyst, [Mn(^{CF3}bpeb)$(OTf)_2$] and assisted for substrate synthesis. M.C. and M.B. directed the experimental part of the project. All authors participated in the writing of the manuscript.

Competing interests:
Authors declare that they have no competing interests.

Supplementary materials:
Materials and methods describing preparation of substrates, characterization of isolated oxidation products and experimental procedures for the catalytic reactions; supplementary text, figures S1-S3, tables S1-S92 and NMR spectra.